

Laser-induced anti-Stokes fluorescence cooling of ytterbium-doped silica glass by more than 6 Kelvin

MOSTAFA PEYSOKHAN^{1,2}, SAEID ROSTAMI¹, ESMAEIL MOBINI^{1,2}, ALEXANDER R. ALBRECHT¹, STEFAN KUHN³, SIGRUN HEIN³, CHRISTIAN HUPEL³, JOHANNES NOLD³, NICOLETTA HAARLAMMERT³, THOMAS SCHREIBER³, RAMONA EBERHARDT³, ANGEL S. FLORES⁴, ANDREAS TÜNNERMANN^{3,5}, MANSOOR SHEIK-BAHAE¹, AND ARASH MAFI^{1,2,*}

¹Department of Physics & Astronomy, University of New Mexico, Albuquerque, New Mexico 87131, USA

²Center for High Technology Materials, University of New Mexico, Albuquerque, New Mexico 87106, USA

³Fraunhofer Institute for Applied Optics and Precision Engineering, Albert-Einstein-Str. 7, 07745 Jena, Germany

⁴Air Force Research Laboratory, Directed Energy Directorate, 3550 Aberdeen Ave. SE, Kirtland Air Force Base, New Mexico 87117, USA

⁵Institute of Applied Physics, Abbe Center of Photonics, Friedrich-Schiller-Universität, Albert-Einstein-Str. 15, 07745 Jena, Germany

*Corresponding author: mafi@unm.edu

Compiled November 24, 2020

Laser cooling of a solid is achieved when a coherent laser illuminates the material, and the heat is extracted by resulting anti-Stokes fluorescence. Over the past year, net solid-state laser cooling was successfully demonstrated for the first time in Yb-doped silica glass in both bulk samples and fibers. Here, we improve the previously published results by one order of magnitude and report more than 6K of cooling below the ambient temperature. This result is the lowest temperature achieved in solid-state laser cooling of silica glass to date to the best of our knowledge. We present details on the experiment performed using a 20W laser operating at 1035nm wavelength and temperature measurements using both a thermal camera and the differential luminescence thermometry technique. © 2020 Optical Society of America

<http://dx.doi.org/10.1364/ao.XX.XXXXXX>

1. INTRODUCTION

The possibility of heat extraction from materials via anti-Stokes fluorescence (ASF) was first suggested by Pringsheim in 1929 [1]. Nearly seven decades later, in 1995, Epstein et al. reported the first experimental observation of laser-induced ASF cooling of a solid in Yb-doped ZBLANP (ZrF_4 – BaF_2 – LaF_3 – AlF_3 – NaF – PbF_2) [2]. Several attempts have since confirmed laser cooling in various solid-state materials, primarily in rare-earth-doped (RE-doped) crystals and glasses. Laser cooling of RE-doped crystals has been the most successful so far [3–5]; the record cooling of a Yb-doped YLiF_4 (Yb:YLF) crystal was reported at the University of New Mexico in 2016 [6]. Several RE-doped glasses have been successfully cooled over the years [7–14]; Yb-doped silica glasses are the most recent additions to the list of successfully cooled RE-doped materials [15–18]. Although laser-cooling of RE-doped silica was thought to be elusive over the years, recent investigations pointed out its possibility [19–21] and eventually led to its experimental observation [15–18, 22–24]. In all these reports, the temperature drop of the laser-cooled Yb-doped silica was less than 1 K. Here we present, to the best of our knowledge, the lowest temperature achieved so far in laser cooling of Yb-doped silica glass by more than 6 K.

There are many potential applications for optical cooling through ASF. In principle, it can be used for compact, vibration-free refrigeration systems [5, 7], e.g., when precision cooling is demanded in low-thermal-noise detectors and reference cavities of ultra-stable lasers, or even in physiological applications [25]. One can even envision laser-cooled silica's potential usage as the substrate in silicon photonics devices [26–29]. Another important potential application for ASF cooling is in radiation-balanced fiber lasers (RBFLs), where anti-Stokes fluorescence cooling balances the waste heat generated in the laser [30–35]. Historically, RE-doped ZBLAN glasses have been more amenable to the stringent requirements needed for laser cooling. Unfortunately, ZBLAN fibers are low in mechanical durability and chemical stability and hard to cleave and splice, so they are generally less desirable than silica fibers. However, the recent advances in laser cooling of Yb-doped silica glass open a potential pathway for future application in RBFLs. Of course, much more substantial cooling is required to make a viable impact on fiber laser designs; this paper is a step in that direction.

2. REVIEW OF THE RECENT RESULTS

The cooling efficiency, η_c , characterizes the potential of a material to cool via laser-induced anti-Stokes fluorescence. It is defined

as the net power density (per unit volume) extracted from the material (p_{net}) per unit total absorbed power density (p_{abs}). The cooling efficiency is a function of the pump laser wavelength λ_p and can be expressed as [16]

$$\eta_c(\lambda_p) = \frac{p_{\text{net}}}{p_{\text{abs}}} = \frac{\lambda_p}{\lambda_f} \eta_{\text{ext}} \eta_{\text{abs}}(\lambda_p) - 1. \quad (1)$$

The mean fluorescence wavelength is represented as λ_f . The external quantum efficiency, η_{ext} , and the absorption efficiency, η_{abs} , are defined as:

$$\eta_{\text{ext}} = \frac{\eta_e W_r}{\eta_e W_r + W_{\text{nr}}}, \quad \eta_{\text{abs}}(\lambda_p) = \frac{\alpha_r(\lambda_p)}{\alpha_r(\lambda_p) + \alpha_b}, \quad (2)$$

where W_r and W_{nr} are radiative and non-radiative decay rates of the excited state in RE dopant, respectively, and η_e is the fluorescence extraction efficiency. α_b is the background absorption coefficient and $\alpha_r(\lambda_p)$ is the resonant absorption coefficient due to the RE dopants. Note that the attenuation due to scattering, including Rayleigh scattering, does not contribute to the material's heating; therefore, α_b represents only the background absorption and not the total parasitic attenuation.

For net solid-state optical refrigeration, the cooling efficiency must be positive; therefore, we must show that $\eta_c > 0$ is reachable over a range of λ_p . The laser pump wavelength λ_p cannot be much longer than λ_f ; otherwise, the pump absorption cross-section would become too small. This would result in a small α_r and hence a small η_{abs} and a negative cooling efficiency. In practice, to observe net cooling, λ_p can only be slightly longer than λ_f , and both η_{ext} and η_{abs} must be near unity. To realize the $\eta_{\text{abs}} \sim 1$ limit for $\lambda_p \gtrsim \lambda_f$, one must increase the RE dopant density to achieve $\alpha_r(\lambda_p) \gg \alpha_b$. However, increasing the RE dopant density results in an increase in the non-radiative decay rate, W_{nr} , primarily because of the RE clustering and quenching, hence decreasing the external quantum efficiency, η_{ext} . This unfortunate circle of undesirable influences was recently overcome in Yb-doped silica—it was shown that by adding certain modifiers such as Al, P, F, and Ce, the quenching concentration of silica glass could be increased significantly [19, 36, 37]. The result was the successful cooling of high-Yb-concentration silica as a fiber preform by Mobini et al. [15, 16] up to 0.7 K, and as an optical fiber by Knall et al. [17] up to 50 mK.

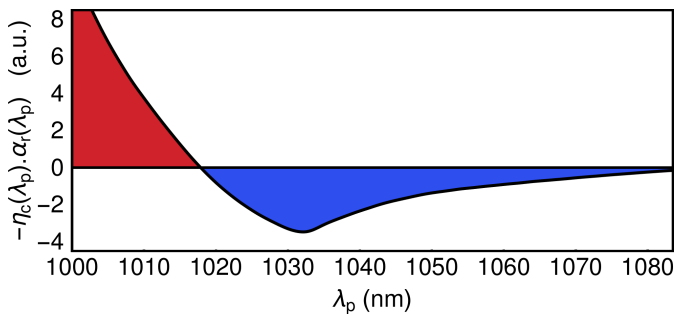


Fig. 1. This figure shows the value of $-\eta_c \alpha_r(\lambda)$, which is proportional to ΔT at a fixed input laser power (in the low-absorption regime), versus the pump laser wavelength for our sample.

To investigate the cooling efficiency as a function of the pump wavelength and obtain the optimum value of λ_p for maximum cooling, we performed laser-induced thermal modulation

Table 1. Properties of the Yb-doped silica glass sample

Parameter	Value	Error
Codopants	Al, P	-
Yb ₂ O ₃ [mol%]	0.12	±0.01
Yb density [10 ²⁵ m ⁻³]	5.3	±0.4
OH ⁻ concentration [ppm]	3.0	±0.5
Core diameter [mm]	1.7	±0.1
Cladding diameter [mm]	2.9	±0.1
Length [mm]	15.1	±0.1
α_b [dB km ⁻¹]	10	±2

spectroscopy (LITMoS) test [5, 38] on our Yb-doped silica samples [16]. In Fig. 1, we show $-\eta_c \alpha_r$ as a function of λ_p for the sample used in this paper (same as sample A in Ref. [16] but some of the cladding is removed; see Table 1). This quantity is proportional to the change in the sample temperature for a fixed pump laser power. Figure 1 shows that the maximum temperature drop can be obtained at around 1035 nm. At the time when we carried out our experiments for Refs. [15, 16], the only viable high-power source in our laboratory was a 1053 nm laser. In this paper, as we will explain later, we are using a $\lambda_p = 1035$ nm source to achieve a higher temperature drop.

3. POWER COOLING EXPERIMENT

The samples that we laser-cooled in our experiments reported in Refs. [15, 16] were surrounded by undoped (no Yb-doping) silica glass cladding regions, which provides significant thermal load. The cooling in our experiments was achieved in spite of this large thermal load. For this work, we chose sample A used in Ref. [16] and removed most of its undoped cladding region to reduce the thermal load and enhance the cooling effect. Moreover, we built a high-power source at the optimum cooling wavelength of 1035 nm as described below.

The characteristics of the (fiber preform) sample are listed in Table 1. The Yb₂O₃ concentration is measured by electron probe micro-analysis. The Yb density is calculated from the measured Yb₂O₃ concentration. The error for the Yb₂O₃ concentration is related to the applied method's uncertainty in this concentration range. OH⁻ concentration and parasitic background absorption (α_b) are measured by the cut-back method in the fiber form, for which the errors express the repeatability of the measurement setup.

To make a high-power source at the nearly optimum $\lambda_p = 1035$ nm wavelength, we have designed and built a fiber amplifier to amplify the output of our continuous-wave tunable Ti:Sapphire laser. The fiber amplifier's gain medium is a 1.2 m piece of Yb-doped double-cladding fiber pumped by a high-power diode laser at the wavelength of 976 nm. The amplifier's input is approximately 300 mW, and the amplified output of the fiber amplifier is on the order of ~ 20 W at 1035 nm wavelength. We note that any residual diode pump power at the 976 nm wavelength can be a significant source of heating in the material because the Yb-silica sample's absorption peaks at 976 nm. Therefore to observe laser cooling, a spectrally pure laser light is essential. To reduce the fiber amplifier's 976 nm pump leakage in the output as much as possible, we implement a cladding

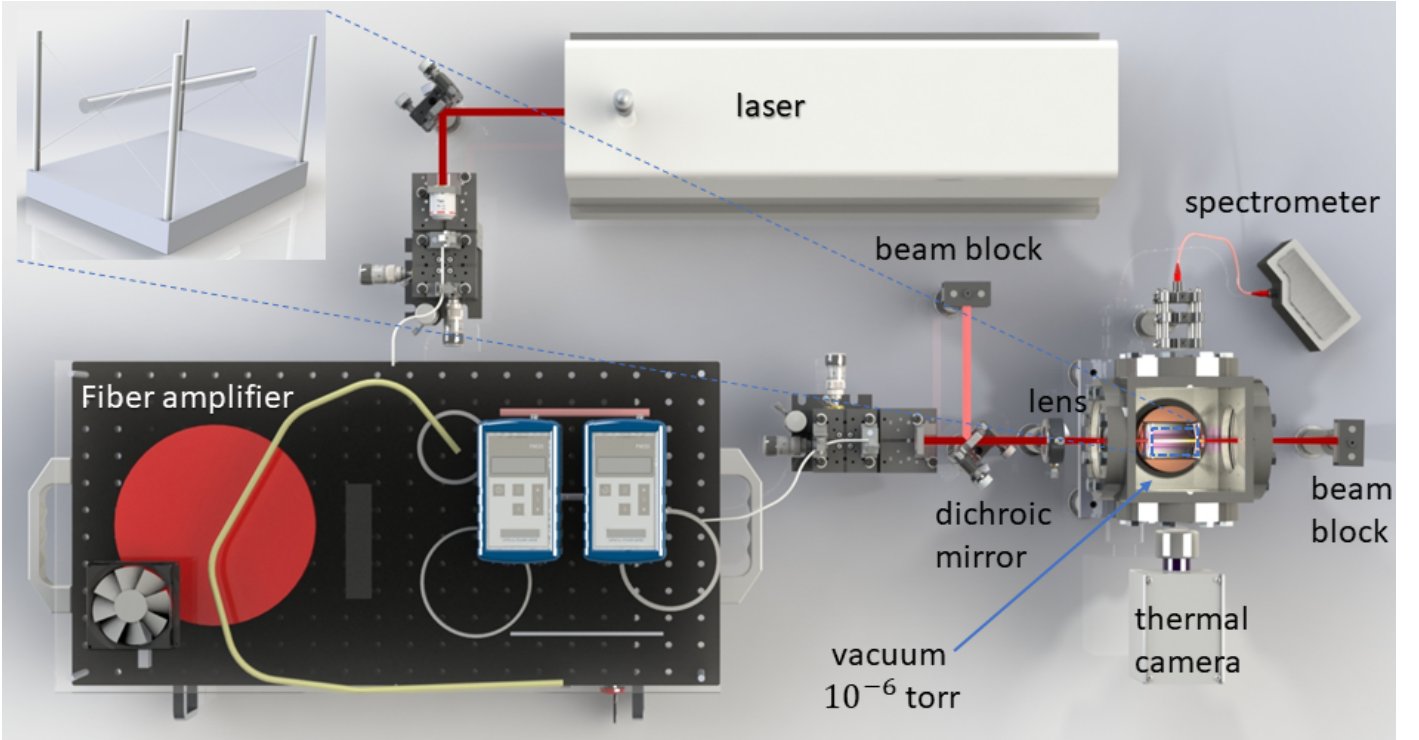


Fig. 2. A wavelength-tunable continuous-wave Ti:Sapphire laser is coupled to a homemade fiber amplifier's input through a 20X microscope objective. The amplified laser light is collimated again by a lens with the focal length of $f=5$ cm. The collimated light is then filtered by a stack of two one-micron long-pass dichroic mirrors. The filtered and collimated light is coupled to the Yb-doped silica glass sample by a lens with the focal length of $f=12$ cm. The sample is held inside a vacuum chamber. The upper-left inset shows a sketch of the Yb-doped silica glass sample supported by a set of thin silica fibers to minimize the heat load.

mode stripper scheme at the fiber amplifier's end. We also use a stack of two 1000 nm wavelength long-pass dichroic mirrors to filter out the rest of the 976 nm pump leakage.

The experimental setup for the power cooling experiment is shown in Fig. 2. The Ti:Sapphire laser is tuned to 1035 nm wavelength, which is then amplified by the fiber amplifier. The output laser light is then collimated and filtered. The collimated light is coupled to the sample through a long-focal-length lens from the outside of the vacuum chamber. The vacuum chamber pressure is maintained at 10^{-6} torr during the power cooling experiment to minimize the convective heat transfer. A spectrometer captures the sample's fluorescence through a KCl salt window mounted in the chamber. Likewise, the thermal images are recorded via a thermal camera through the thermally transparent KCl salt window, and the images are post-processed to measure the changes in the sample's temperature [16]. The mean fluorescence wavelength is calculated from the fluorescence emission measured by an optical spectrum analyzer and is found to be $\lambda_f = 1010$ nm. In order to decrease the thermal contact on the sample, the sample is mounted on very thin glass fibers. To minimize the back-reflection into the fiber amplifier, the sample and chamber windows are tilted slightly, and a beam block is used to capture the laser after exiting the sample.

The red dots in Fig. 3 show the sample's temperature evolution, measured by the thermal camera, as a function of exposure time to the 20 W laser light at 1035 nm. The temperature drop is $\Delta T = T_s - T_0$, where T_s is the sample temperature and $T_0 \approx 23^\circ\text{C}$ is the ambient temperature. The thermal camera saturates at $\Delta T \approx -6$ K, so the temperature may have dropped below the saturation value (see section 4). In this power cooling

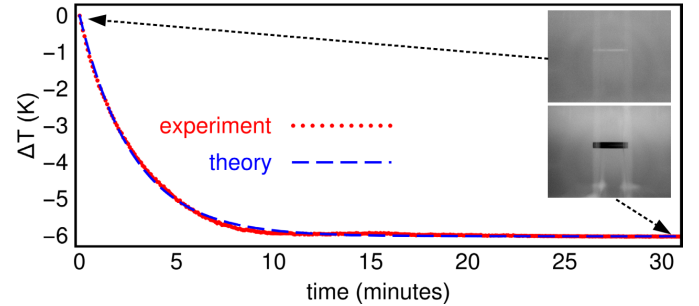


Fig. 3. The sample's temperature change is plotted as a function of time when exposed to the high-power 1035 nm laser light. The red dots correspond to the experimental results, and the blue dashed line represents the fitting of the exponential function in Eq. (3) to the experimental data. The insets show two thermal images corresponding to before laser exposure and after the final temperature stabilization, respectively.

experiment, the sample's temperature evolution as a function of time follows the following exponential form (see Ref. [16] for a derivation):

$$\Delta T(t) = \Delta T_{\max}(e^{-t/\tau_c} - 1), \quad (3)$$

where we use the following definitions:

$$\Delta T_{\max} = \eta_c \frac{P_{\text{abs}}}{4\epsilon\sigma T_0^3 A}, \quad \tau_c = \frac{\rho V c_v}{4\epsilon\sigma T_0^3 A}. \quad (4)$$

V is the sample volume, $\epsilon = 0.85$ is the emissivity of the implemented Yb-doped silica glass fiber preform, $\sigma = 5.67 \times 10^{-8} \text{ W} \cdot \text{m}^{-2} \cdot \text{K}^{-4}$ is the Stefan-Boltzmann constant, T_0 is the ambient temperature, A is the surface area of the sample, $\rho = 2.2 \times 10^3 \text{ kg} \cdot \text{m}^{-3}$ is the silica glass mass density, and $c_v = 741 \text{ J} \cdot \text{kg}^{-1} \cdot \text{K}^{-1}$ is the specific heat of the silica glass. [39–41]. P_{abs} is the absorbed laser power that can be estimated from the Beer-Lambert law in a single pass [42, 43]:

$$P_{\text{abs}} = P_{\text{in}} \left(1 - e^{-\alpha_r(\lambda_p)l}\right) \approx P_{\text{in}}\alpha_r(\lambda_p)l. \quad (5)$$

P_{in} is the input power coupled into the fiber preform at $z = 0$ and l is the sample length. In fact, by combining Eqs. (4) and (5), we can see that $\Delta T_{\text{max}} \propto \eta_c \alpha_r$, which is the vertical axis in Fig. 1 used to estimate the optimum pump laser wavelength. By fitting the exponential form in Eq. (3) to the experimental data (red dots) in Fig. 3, we obtain $\Delta T_{\text{max}} = 6.02 \pm 0.01 \text{ K}$ and $\tau_c \approx 166 \pm 1 \text{ s}$ —the error-bars are estimated by the fitting procedure. The dashed blue line is the theoretical fit and agrees with the experiment quite well. Using the measured value of $\eta_c \approx 0.016$ at $\lambda_p \approx 1035 \text{ nm}$ reported in Ref. [16] for Sample A, we use Eqs. (4) and (5) to estimate $\Delta T_{\text{max}} \approx 9 \text{ K}$. This theoretical estimate is consistent with the measured fitted value of $\Delta T_{\text{max}} = 6.02 \pm 0.01 \text{ K}$, because the heat conduction from the fiber-holder contact and also the parasitic heating from fiber facet imperfections are not included in the theoretically ideal form of Eq. (4). Moreover, the fitted value for τ_c agrees quite well with the measurement reported in Ref. [16], once the difference in geometry is taken into account ($\tau_c \approx 175 \text{ s}$ versus $\tau_c \approx 166 \text{ s}$). The goodness of the fitting in Fig. 3 indicates that despite the saturation of the camera, the actual value of ΔT_{max} cannot be much larger than 6 K.

4. DIFFERENTIAL LUMINESCENCE THERMOMETRY

The thermal camera that we use in our experiments gets saturated at around 6 K below the ambient temperature and the pixels become black. To cross-check the temperature measurements and see if the sample temperature drops more than 6 K below the ambient temperature, we use an alternative temperature measurement method dubbed as Differential Luminescence Thermometry (DLT). In this technique, the variation in luminescence intensity distribution with temperature is used to determine the sample’s temperature. This variation is due to the temperature-dependence of the Boltzmann population of the crystal field levels of the emitting state and the homogeneous linewidth of the individual crystal field transitions [44]. DLT has been successfully used to measure temperature variations on the order of tens of Kelvin [6]; however, it can be quite noisy and less accurate for smaller temperature variations such as those reported here. The reason is that unlike semiconductors where substantial spectral shifts are observed as a function of the temperature [45], the 4f electrons in REs are shielded from the environment in a solid.

For DLT, the temperature-dependent emission spectral density $S(\lambda, T)$ is obtained in real-time and is referenced to a spectrum at the starting temperature T_0 . The normalized differential spectrum is defined as:

$$\Delta S(\lambda, T, T_0) = \frac{S(\lambda, T)}{S_{\text{max}}(T)} - \frac{S(\lambda, T_0)}{S_{\text{max}}(T_0)}. \quad (6)$$

Normalization to the spectral peak S_{max} is performed to eliminate the effect of input power fluctuations. The scalar DLT signal

is given by

$$S_{\text{DLT}}(T, T_0) = \int_{\lambda_1}^{\lambda_2} d\lambda |\Delta S(\lambda, T, T_0)|, \quad (7)$$

where the limits of integration bracket the sample’s spectral emission, eliminating possible contributions from the spurious laser line scattering; we choose $\lambda_1 = 895 \text{ nm}$ and $\lambda_2 = 955 \text{ nm}$. The temperature drop from the ambient, ΔT , is linearly proportional to S_{DLT} : $\Delta T = \gamma \cdot S_{\text{DLT}}$, where γ is the proportionality constant. To use DLT for temperature measurements, we first perform a calibration measurement by mounting the sample on a variable-temperature cold plate while pumping the sample with the Ti:Sapphire laser and collecting the spectrum. We find that for our sample $\gamma = -34 \pm 2 \text{ K}$.

We use the DLT calibration result to measure the sample’s temperature evolution over time while being exposed to the 20 W laser light at 1035 nm by collecting the emission spectral density every ten seconds. The results are shown in Fig. 4. The DLT data points are in blue dots where the error-bars are due to the error in γ as estimated from the calibration. The results are compared with the thermal camera measurements in red dots. The DLT results are quite noisy as expected; however, the trend agrees with the temperature values from the thermal camera and also hint that the sample is cooled slightly more than 6 K below the ambient temperature, consistent with the results presented in the previous section.

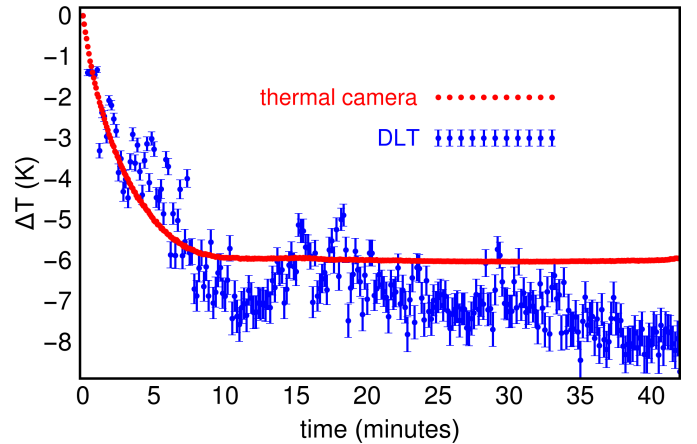


Fig. 4. The sample’s temperature change is plotted as a function of time when exposed to the high-power 1035 nm laser light. The blue dots are based on the DLT method and the red dots represent the temperature measurements using the thermal camera.

5. CONCLUSIONS

Here we present, to the best of our knowledge, the lowest temperature achieved so far in laser cooling of Yb-doped silica glass by more than 6 K. This result constitutes almost an order of magnitude improvement compared with the previous result of 0.7 K reported by Mobini et al. [15, 16]. The improvement was achieved by using a laser light at the near-optimal wavelength of 1035 nm (rather than 1053 nm), nearly doubling the pump power to 20 W, and reducing the undoped cladding diameter of the fiber preform from 10.7 mm to 2.9 mm hence decreasing the thermal load. Future improvements are possible by increasing the pump power and implementing a multi-pass scheme, and

improving material specifications. A video clip of the cooling evolution of the sample is presented as the Supplementary. The video shows the temporal evolution of the sample's temperature as captured by the thermal camera in the high-power laser cooling experiment. The thermal image of the sample gets darker as the sample cools due to the exposure to high-power laser.

FUNDING

This material is based upon work supported by the Air Force Office of Scientific Research under award number FA9550-16-1-0362 titled Multidisciplinary Approaches to Radiation Balanced Lasers (MARBLE).

ACKNOWLEDGMENTS

The authors would like to acknowledge R. I. Epstein, M. P. Hehlen, and S. D. Melgaard for helpful discussions.

AUTHOR CONTRIBUTIONS

M.P. and A.M. wrote the manuscript and all authors contributed to its final editing. M.P., A.A. and S.R. conducted all the experiments and analyzed the data; S.K., S.H., C.H., J.N., N.H., T.S., and R.E. are responsible for the production and characterization of the silica glass preforms and A.T. supervised their work. A.F. and E.M. helped in making the fiber amplifier. A.M. and M.S.-B. led and supervised the laser cooling aspects of the work and participated in the data analysis.

Disclosures. The authors declare no conflicts of interest.

REFERENCES

- P. Pringsheim, "Zwei bemerkungen über den unterschied von lumineszenz-und temperaturstrahlung," *Z. Phys.* **57**, 739–746 (1929).
- R. I. Epstein, M. I. Buchwald, B. C. Edwards, T. R. Gosnell, and C. E. Mungan, "Observation of laser-induced fluorescent cooling of a solid," *Nature* **377**, 500–503 (1995).
- D. V. Seletskiy, S. D. Melgaard, S. Bigotta, A. Di Lieto, M. Tonelli, and M. Sheik-Bahae, "Laser cooling of solids to cryogenic temperatures," *Nat. Photonics* **4**, 161–164 (2010).
- G. Nemova and R. Kashyap, "Laser cooling of solids," *Rep. Prog. Phys.* **73**, 086501 (2010).
- D. V. Seletskiy, R. Epstein, and M. Sheik-Bahae, "Laser cooling in solids: advances and prospects," *Rep. Prog. Phys.* **79**, 096401 (2016).
- S. D. Melgaard, A. R. Albrecht, M. P. Hehlen, and M. Sheik-Bahae, "Solid-state optical refrigeration to sub-100 Kelvin regime," *Sci. Rep.* **6**, 20380 (2016).
- T. R. Gosnell, "Laser cooling of a solid by 65 k starting from room temperature," *Opt. Lett.* **24**, 1041–1043 (1999).
- J. Fernández, A. Mendioroz, A. J. García, R. Balda, and J. L. Adam, "Anti-Stokes laser-induced internal cooling of yb^{3+} -doped glasses," *Phys. Rev. B* **62**, 3213–3217 (2000).
- C. Hoyt, M. Sheik-Bahae, R. Epstein, B. Edwards, and J. Anderson, "Observation of anti-Stokes fluorescence cooling in thulium-doped glass," *Phys. Rev. Lett.* **85**, 3600 (2000).
- J. Thiede, J. Distel, S. Greenfield, and R. Epstein, "Cooling to 208 K by optical refrigeration," *Appl. Phys. Lett.* **86**, 154107 (2005).
- J. Fernandez, A. J. Garcia-Adeva, and R. Balda, "Anti-Stokes laser cooling in bulk erbium-doped materials," *Phys. review letters* **97**, 033001 (2006).
- D. T. Nguyen, R. Thapa, D. Rhonehouse, J. Zong, A. Miller, G. Hardesty, N.-H. Kwong, R. Binder, and A. Chavez-Pirson, "Towards all-fiber optical coolers using Tm-doped glass fibers," in *Laser Refrigeration of Solids VI*, vol. 8638 (International Society for Optics and Photonics, 2013), p. 86380G.
- M. Peysokhan, E. Mobini, and A. Mafi, "Measuring the anti-Stokes cooling parameters of a Bb-doped ZBLAN fiber for radiation balancing," in *Sixth International Workshop on Specialty Optical Fibers and Their Applications (WSOF 2019)*, vol. 11206 (2019), pp. 112061Q–1.
- M. Peysokhan, E. Mobini, A. Allahverdi, B. Abaie, and A. Mafi, "Characterization of Yb-doped ZBLAN fiber as a platform for radiation-balanced lasers," *Photonics Res.* **8**, 202–210 (2020).
- E. Mobini, S. Rostami, M. Peysokhan, A. Albrecht, S. Kuhn, S. Hein, C. Hupel, J. Nold, N. Haarlammer, T. Schreiber *et al.*, "Laser cooling of silica glass," arXiv preprint arXiv:1910.10609 (2019).
- E. Mobini, S. Rostami, M. Peysokhan, A. Albrecht, S. Kuhn, S. Hein, C. Hupel, J. Nold, N. Haarlammer, T. Schreiber *et al.*, "Laser cooling of ytterbium-doped silica glass," *Commun. Phys.* **3**, 134 (2020).
- J. Knall, P.-B. Vigneron, M. Engholm, P. D. Dragic, N. Yu, J. Ballato, M. Bernier, and M. J. F. Digonnet, "Laser cooling in a silica optical fiber at atmospheric pressure," *Opt. Lett.* **45**, 1092–1095 (2020).
- J. Knall, M. Engholm, J. Ballato, P. D. Dragic, N. Yu, and M. J. F. Digonnet, "Experimental comparison of silica fibers for laser cooling," *Opt. Lett.* **45**, 4020–4023 (2020).
- E. Mobini, M. Peysokhan, B. Abaie, M. P. Hehlen, and A. Mafi, "Spectroscopic investigation of Yb-doped silica glass for solid-state optical refrigeration," *Phys. Rev. Appl.* **11**, 014066 (2019).
- J. M. Knall, A. Arora, P. D. Dragic, J. Ballato, M. Cavillon, T. Hawkins, S. Jiang, T. Luo, M. Bernier, and M. Digonnet, "Experimental investigations of spectroscopy and anti-Stokes fluorescence cooling in Yb-doped silicate fibers," in *Photonic Heat Engines: Science and Applications*, vol. 10936 D. V. Seletskiy, R. I. Epstein, and M. Sheik-Bahae, eds., International Society for Optics and Photonics (SPIE, 2019), pp. 40–49.
- E. Mobini, M. Peysokhan, B. Abaie, and A. Mafi, "Investigation of solid state laser cooling in ytterbium-doped silica fibers," in *2018 Conference on Lasers and Electro-Optics (CLEO)*, (2018), pp. 1–2.
- E. Mobini, S. Rostami, M. Peysokhan, A. R. Albrecht, S. Kuhn, S. Hein, C. Hupel, J. Nold, N. Haarlammer, T. Schreiber, R. Eberhardt, A. Tünnermann, M. Sheik-Bahae, and A. Mafi, "Observation of anti-Stokes fluorescence cooling of ytterbium-doped silica glass (Conference Presentation)," in *Photonic Heat Engines: Science and Applications II*, vol. 11298 D. V. Seletskiy, R. I. Epstein, and M. Sheik-Bahae, eds., International Society for Optics and Photonics (SPIE, 2020).
- J. M. Knall, P.-B. Vigneron, M. Engholm, P. D. Dragic, N. Yu, J. Ballato, M. Bernier, and M. Digonnet, "Experimental observation of cooling in Yb-doped silica fibers," in *Photonic Heat Engines: Science and Applications II*, vol. 11298 D. V. Seletskiy, R. I. Epstein, and M. Sheik-Bahae, eds., International Society for Optics and Photonics (SPIE, 2020), pp. 48–55.
- J. Knall, M. Engholm, J. Ballato, P. D. Dragic, N. Yu, and M. J. F. Digonnet, "Experimental comparison of silica fibers for laser cooling," *Opt. Lett.* **45**, 4020–4023 (2020).
- X. Zhou, B. E. Smith, P. B. Roder, and P. J. Pauzauskie, "Laser refrigeration of ytterbium-doped sodium–yttrium–fluoride nanowires," *Adv. Mater.* **28**, 8658–8662 (2016).
- X. Zhu and N. Peyghambarian, "High-power ZBALN glass fiber lasers: review and prospect," *Adv. Optoelectron.* **2010** (2010).
- E. Mobini, M. Peysokhan, and A. Mafi, "Heat mitigation of a core/cladding Yb-doped fiber amplifier using anti-Stokes fluorescence cooling," *J. Opt. Soc. Am. B* **36**, 2167–2177 (2019).
- B. Jalali and S. Fathpour, "Silicon photonics," *J. Light. Technol.* **24**, 4600–4615 (2006).
- R. Soref, "Mid-infrared photonics in silicon and germanium," *Nat. Photonics* **4**, 495–497 (2010).
- S. R. Bowman, "Lasers without internal heat generation," *IEEE J. Quant. Electron.* **35**, 115–122 (1999).
- G. Nemova and R. Kashyap, "Athermal continuous-wave fiber amplifier," *Opt. Commun.* **282**, 2571–2575 (2009).
- S. R. Bowman, S. P. O'Connor, S. Biswal, N. J. Condon, and A. Rosenberg, "Minimizing heat generation in solid-state lasers," *IEEE J. Quant. Electron.* **46**, 1076–1085 (2010).
- G. Nemova and R. Kashyap, "Radiation-balanced amplifier with two

- pumps and a single system of ions," J. Opt. Soc. Am. B **28**, 2191–2194 (2011).
34. E. Mobini, M. Peysokhan, B. Abaie, and A. Mafi, "Thermal modeling, heat mitigation, and radiative cooling for double-clad fiber amplifiers," J. Opt. Soc. Am. B **35**, 2484–2493 (2018).
 35. Z. Yang, J. Meng, A. R. Albrecht, and M. Sheik-Bahae, "Radiation-balanced Yb:YAG disk laser," Opt. Express **27**, 1392–1400 (2019).
 36. J. Lægsgaard, "Dissolution of rare-earth clusters in SiO₂ by Al codoping: a microscopic model," Phys. Rev. B **65**, 174114 (2002).
 37. K. Arai, H. Namikawa, K. Kumata, T. Honda, Y. Ishii, and T. Handa, "Aluminum or phosphorus co-doping effects on the fluorescence and structural properties of neodymium-doped silica glass," J. Appl. Phys. **59**, 3430–3436 (1986).
 38. S. Rostami, A. R. Albrecht, A. Volpi, and M. Sheik-Bahae, "Observation of optical refrigeration in a holmium-doped crystal," Photonics Res. **7**, 445–451 (2019).
 39. P. Yoder, D. Vukobratovich, and R. A. Paquin, *Opto-mechanical systems design, 2nd Ed.* (CRC press, New York, 1992).
 40. M. Karimi, "Theoretical study of the thermal distribution in Yb-doped double-clad fiber laser by considering different heat sources," Prog. Electromagn. Res. **88**, 59–76 (2018).
 41. A. Mafi, "Temperature distribution inside a double-cladding optical fiber laser or amplifier," J. Opt. Soc. Am. B **37**, 1821–1828 (2020).
 42. R. C. Powerl, "Physics of solid-state laser materials," (Springer, New York, 1998).
 43. M. Peysokhan, E. Mobini, B. Abaie, and A. Mafi, "Method for measuring the resonant absorption coefficient of rare-earth-doped optical fibers," Appl. Opt. **58**, 1841–1846 (2019).
 44. W. M. Patterson, D. V. Seletskiy, M. Sheik-Bahae, R. I. Epstein, and M. P. Hehlen, "Measurement of solid-state optical refrigeration by two-band differential luminescence thermometry," J. Opt. Soc. Am. B **27**, 611–618 (2010).
 45. B. Imangholi, M. P. Hasselbeck, D. A. Bender, C. Wang, M. Sheik-Bahae, R. I. Epstein, and S. Kurtz, "Differential luminescence thermometry in semiconductor laser cooling," in *Physics and Simulation of Optoelectronic Devices XIV*, vol. 6115 M. Osinski, F. Henneberger, and Y. Arakawa, eds., International Society for Optics and Photonics (SPIE, 2006), pp. 215 – 220.